Journal of Alloys and Compounds 509 (2011) 7439–7446

Contents lists available at ScienceDirect

Journal of Alloys and Compounds

journal homepage: www.elsevier.com/locate/jallcom

Synthesis and characterization of Cu_2ZnSnS_4 thin films grown by PLD: Solar cells

A.V. Moholkar[a,b,*], S.S. Shinde[a], A.R. Babar[a], Kyu-Ung Sim[b], Hyun Kee Lee[b], K.Y. Rajpure[a], P.S. Patil[c], C.H. Bhosale[a], J.H. Kim[b,**]

[a] Electrochemical Materials Laboratory, Department of Physics, Shivaji University, Kolhapur 416004, India
[b] Department of Materials Science and Engineering, Chonnam National University, 300 Yongbong-Dong, Puk-Gu, Gwangju 500-757, South Korea
[c] Thin Film Laboratory, Department of Physics, Shivaji University, Kolhapur 416004, India

ARTICLE INFO

Article history:
Received 14 March 2011
Received in revised form 10 April 2011
Accepted 14 April 2011
Available online 21 April 2011

Keywords:
CZTS
PLD
Structural
XPS
Optical properties
Device

ABSTRACT

As-deposited and annealed Cu_2ZnSnS_4 (CZTS) thin films have been synthesized onto Mo coated glass substrates at different deposition times using pulsed laser deposition (PLD) technique. The effect of deposition time (film thickness) and annealing onto the structural, morphological, compositional and optical properties of CZTS thin films have been investigated. The polycrystalline CZTS thin films with tetragonal crystal structure have been observed from structural analysis. FESEM and AFM images show the smooth, uniform, homogeneous and densely packed grains and increase in the grain size after annealing. The internal quantitative analysis has been carried out by XPS study which confirms the stoichiometry of the films. The optical band gap of CZTS films grown by PLD is about 1.54 eV, which suggests that CZTS films can be useful as an absorber layer in thin film solar cells. Device performance for deposited CZTS films has been studied.

1. Introduction

The modern world's facilities are mainly dependent on electricity and henceforth the progress is ultimately based on the pillars of energy apart from the currencies. Since the world is propagating on the different energy strategies, it is necessary to fabricate high conversion efficiency solar cells without material degradation. Therefore the study of low cost solar cells has become popular in many countries. The Cu_2ZnSnS_4 (CZTS) film possesses the optimal characteristics like the band gap energy of 1.4–1.5 eV and absorption coefficient of $10^4\,cm^{-1}$ required for fabrication of thin film solar cell (TFSC). The commercial production based on the CZTS absorber layer is purposely studied [1,2]. Further CZTS is cheap and does not contain any toxic elements such as Se or Cd, leading to a solar cell with less environmental damage and low capital cost, which is very essential as far as the practical application on the broad band scale, is concerned.

The synthesis of single-crystal CZTS was first reported by Nitsche et al. wherein the crystal growth was carried out using the iodine vapour transport method [3]. Ito and Nakazawa [1] reported the photovoltaic effect in the heterojunction diode using sputtered CZTS thin films and cadmium tin oxide for the first time. As compared to Cu_2InGeS_4 (CIGS) solar cell, the research oriented study on the application of CZTS thin films is still insufficient and needs more systematic investigations to increase the conversion efficiency. A variety of physical and chemical techniques have been employed to deposit CZTS thin films including co-evaporation [4], electrodeposition [5,6], RF sputtering [7], atom beam sputtering [1], hybrid sputtering [8], RF magnetron sputtering [9], thermal evaporation [10], pulsed laser deposition (PLD) [11–13], sulfurization of electron beam evaporated precursors [14], spray pyrolysis [15] and sol–gel sulfurizing method [16] etc.

Among these, the PLD technique allows preparing all kinds of oxides, nitrides, carbides, and polymers. Additionally in this case, the energy source is outside the deposition chamber. For oxide films, the use of oxygen is often inevitable to have sufficient oxygen in the growing oxide film [17]. Furthermore, the inert gas pressure makes it versatile, as the energy of the deposited particles is a free parameter to play with which can be tuned for special purposes, like an adjustment of texture, stress or interface roughness. The other preparative parameters, such as pulse repetition rate, pulse length, fluencies, target-to-substrate distance, substrate temperature and substrate orientation have a strong influence on film properties which demonstrate the enormous versatility of PLD. The deposition in vivid atmospheres to have good stoichiometric multi component films is also possible [18,19]. The literature survey shows that, in

* Corresponding author at: Electrochemical Materials Laboratory, Department of Physics, Shivaji University, Kolhapur 416004, India. Tel.: +91 0231 2609435; fax: +91 0231 2691533.
** Corresponding author. Tel.: +82 62 530 1709; fax: +82 62 530 1699.
E-mail addresses: avmoholkar@yahoo.co.in (A.V. Moholkar), jinhyeok@chonnam.ac.kr (J.H. Kim).

0925-8388/$ – see front matter © 2011 Elsevier B.V. All rights reserved.
doi:10.1016/j.jallcom.2011.04.074

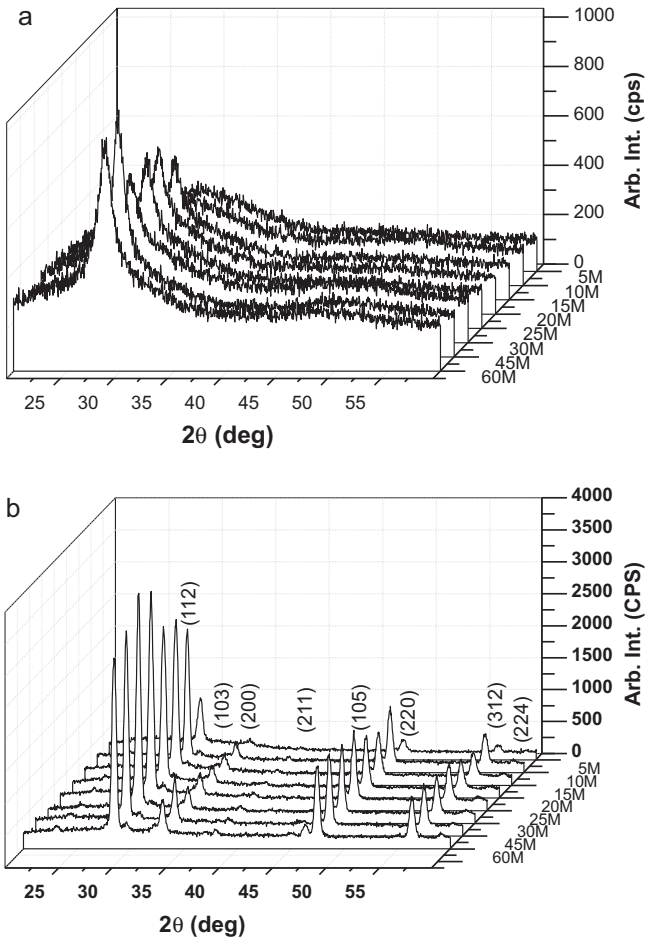

Fig. 1. X-ray diffraction patterns of CZTS thin films for different deposition times (min) (a) as deposited (b) annealed.

spite of having such a fascinating technique for the deposition of thin films, very meagre amount of work on CZTS thin films has been carried out using this method, probably may be due to small area of deposition (usually 1 cm^2) [20–22]. But as an endeavour of improving the solar cell efficiency based on the CZTS absorber layer, we have been focused to study, in detail the effect of each and every process parameters involved in the PLD on film properties.

In this paper, the influence of film thickness of as-deposited and annealed CZTS thin films deposited using various deposition times and its effect on their structural, compositional, optical, surface morphological and chemical properties has been investigated. Further the solar cell developed using this combination Glass/Mo/CZTS/CdS/ZnO:Al/Al has been tested.

2. Experimental

CZTS pellet was used as a target, which was synthesized by the solid state reaction method of Cu_2S, ZnS and SnS_2 powders mixed with 1:1:1 mol ratio. The ball milled compound powder was shaped into a pellet and sealed into an evacuated quartz ampoule, kept at 750 °C for 4 h in a microprocessor based furnace Model 08-F03 (Ajeon, South Korea). The rate of increase and decrease of temperature was 2 °C/min. After room temperature cooling the ampoule was broken and the target was double polished. The Mo coated glass substrates were used for the deposition after ultrasonic cleaning using organic solvents like acetone, methanol, and ethanol then double distilled water for 5 min, consecutively. The deposition was carried out at room temperature. A KrF excimer laser of 248 nm wavelength with 25 ns pulse width (Lambda Physik, LPX305icc) was used for the deposition of CZTS thin films. The deposition chamber was evacuated to 1.5×10^{-5} Torr using a turbo molecular pump. The substrates were placed parallel at distance of 40 mm away from the target, which were fixed on a rotating target holder with rotation of 500 rpm. The other parameters viz. the pulsed laser energy density (2.5 J/cm^2), repetition rate (10 Hz) was kept constant and the deposition time was varied from 5 to 30 min, at the interval of 5 min and then 45 and 60 min, respectively. These films were further annealed in a furnace containing N_2 (95%) + H_2S (5%) atmosphere at 400 °C. The temperature was increased to desired temperature at a rate of 3 °C/min and hold for 1 h. After annealing, the furnace was cooled to room temperature at a rate of 3 °C/min.

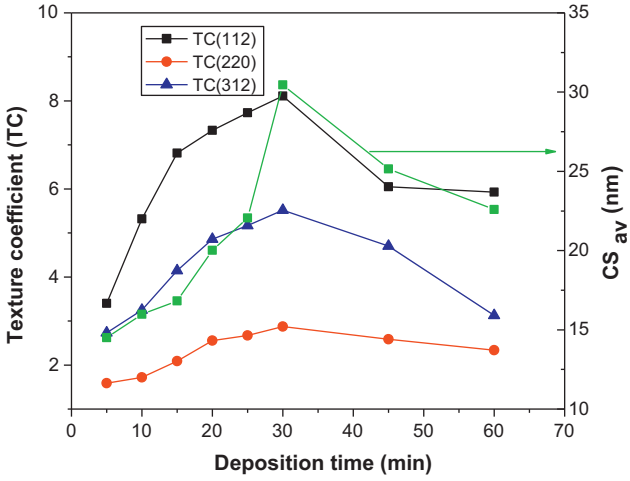

Fig. 2. Variation of TC of (1 1 2), (2 2 0), (3 1 2) peaks and average crystallite size (CS_{av}) with deposition time for CZTS thin films.

The synthesized CZTS films were characterized by XRD, FESEM, AFM, XPS and optical measurements. The structural properties of the as-deposited and annealed thin films were studied using high resolution X-ray diffraction (XRD) with Ni-filtered Cu K_α radiation of 1.54056 Å (X'pert PRO, Philips, Eindhoven, Netherlands). The surface morphology of films was observed by using field emission scanning electron microscopy (FE-SEM, Model: JSM-6701F, UK). The 2D and 3D images along with surface roughness of the films was recorded using atomic force microscopy (AFM, Digital Instrument, nanoscope III, USA). The compositional analysis of the film was carried out using an energy dispersive spectrometer (EDS) system attached to FESEM (JEOL, JSM-7500F, Japan). The determination of the chemical bonding was performed by X-ray photoelectron spectroscopy (XPS, VG Multilab 2000, Thermo VG Scientific, UK) with monochromatic Mg-Kα (1253.6 eV) radiation source. The carbon 1 s line corresponding to 285 eV was used for the calibration of the binding energies in the spectrometer. Deconvolution of XPS peaks was performed using Lorentzing fitting with identical FWHM after Shirley background substraction. Optical absorption study of the films was carried out in the wavelength range of 300–800 nm using UV–Vis–NIR spectrophotometer (Cary 100, Varian, Mulgrave, Australia). The photovoltaic cell of Glass/Mo/CZTS/CdS/ZnO:Al/Al structure was been fabricated. A CdS buffer layer on the CZTS absorber was deposited using a chemical bath deposition (CBD) process. The ZnO:Al window layer [23] was then deposited using an rf sputtering technique. An Al top grid on the ZnO:Al window layer was deposited using a vacuum evaporation method.

3. Results and discussion

The structural analysis of as-deposited and annealed CZTS thin films for various deposition times (5–60 min) is shown in Fig. 1(a and b). It is seen that, as-deposited films with low deposition time (up to 10 min) shows microcrystalline nature. Above 10 min deposition time, transformation of microcrystalline to nanocrystalline crystalline phase for CZTS thin films has observed. The deposited films are slightly polycrystalline in nature having tetragonal crystal structure confirmed with the help of comparison of standard and observed d values using ASTM data card No. 26-0575. CZTS is a tetrahedrally coordinated semiconductor, where each sulfur anion is bonded to four cations and each cation is bonded to four sulfur anions. The ordering of the cations in the cation sublattice may occur by alternate cation layers with sulfur anion layers along the crystallographic c-direction as CuCu/SS/ZnSn/SS [24].

The annealed CZTS films show an increase in the peak intensity for all planes due to enhancement in the crystallinity as compared to as-deposited films. The (1 1 2) strong orientation is observed for all CZTS films with some weak intense peaks such as (1 0 3), (2 0 0), (2 1 1), (1 0 5), (2 2 0), (3 1 2), (2 2 4) etc. The crystallinity increases

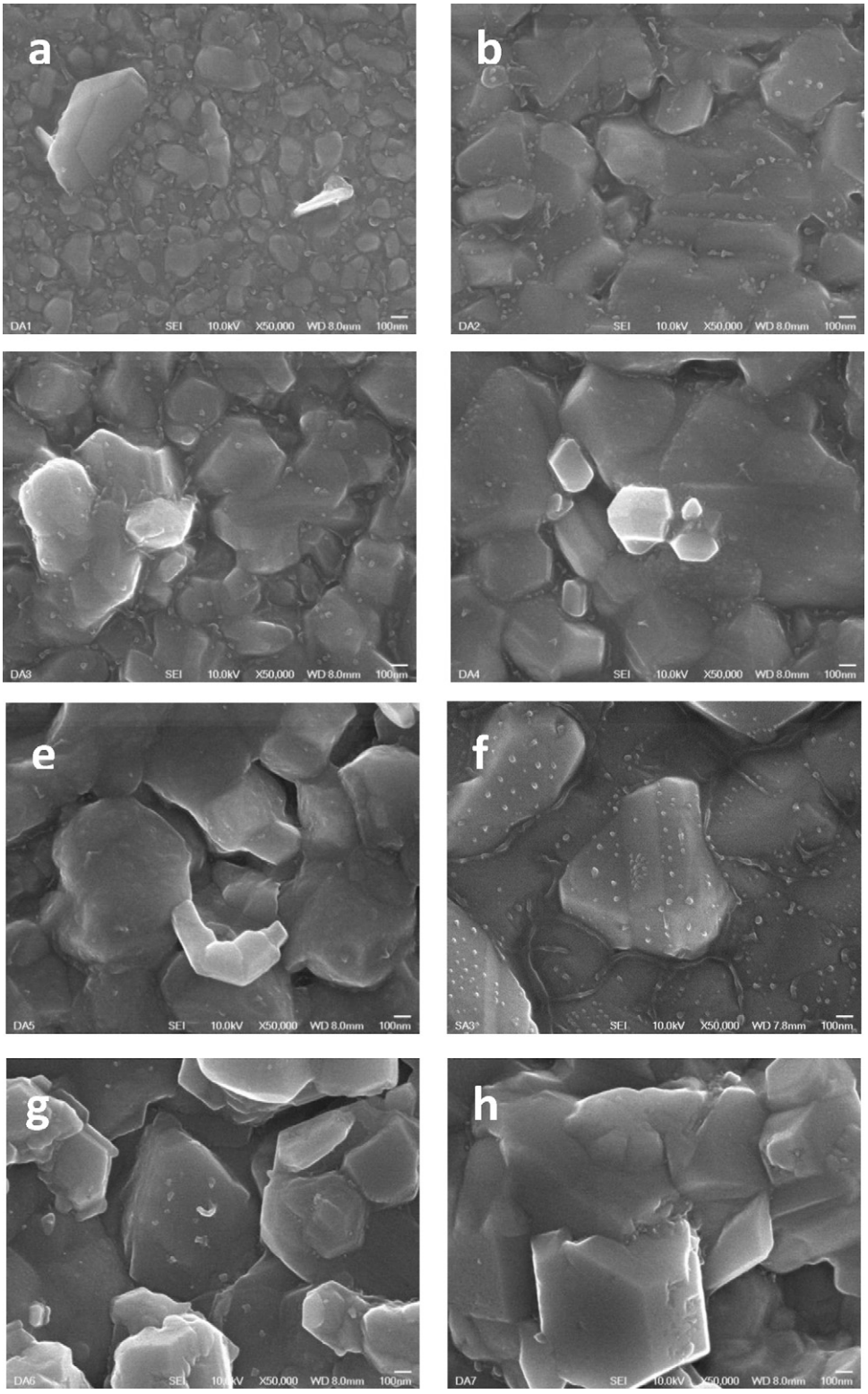

Fig. 3. FE-SEM images of annealed CZTS thin films for various deposition times: (a) 5 min, (b) 10 min (c) 15 min, (d) 20 min, (e) 25 min, (f) 30 min, (g) 45 min and (h) 60 min.

with increase in deposition time up to 30 min and then decreases for higher deposition times. The mobility of deposited atoms on substrate surface might have enhanced due to increase in deposition time; therefore, the crystallinity improves with increasing deposition time up to 30 min. Furthermore, too high deposition time could lead to bulky grains. Therefore, the crystalline quality of film deposited with 45 and 60 min is degraded slightly.

The crystallite size of the films is calculated using the Scherrer's relation,

$$D = \frac{0.9\lambda}{\beta \cos\theta} \quad (1)$$

where D is the diameter of the crystallites forming the film, λ is the wavelength of the Cu-K_α line, β is the FWHM in radians

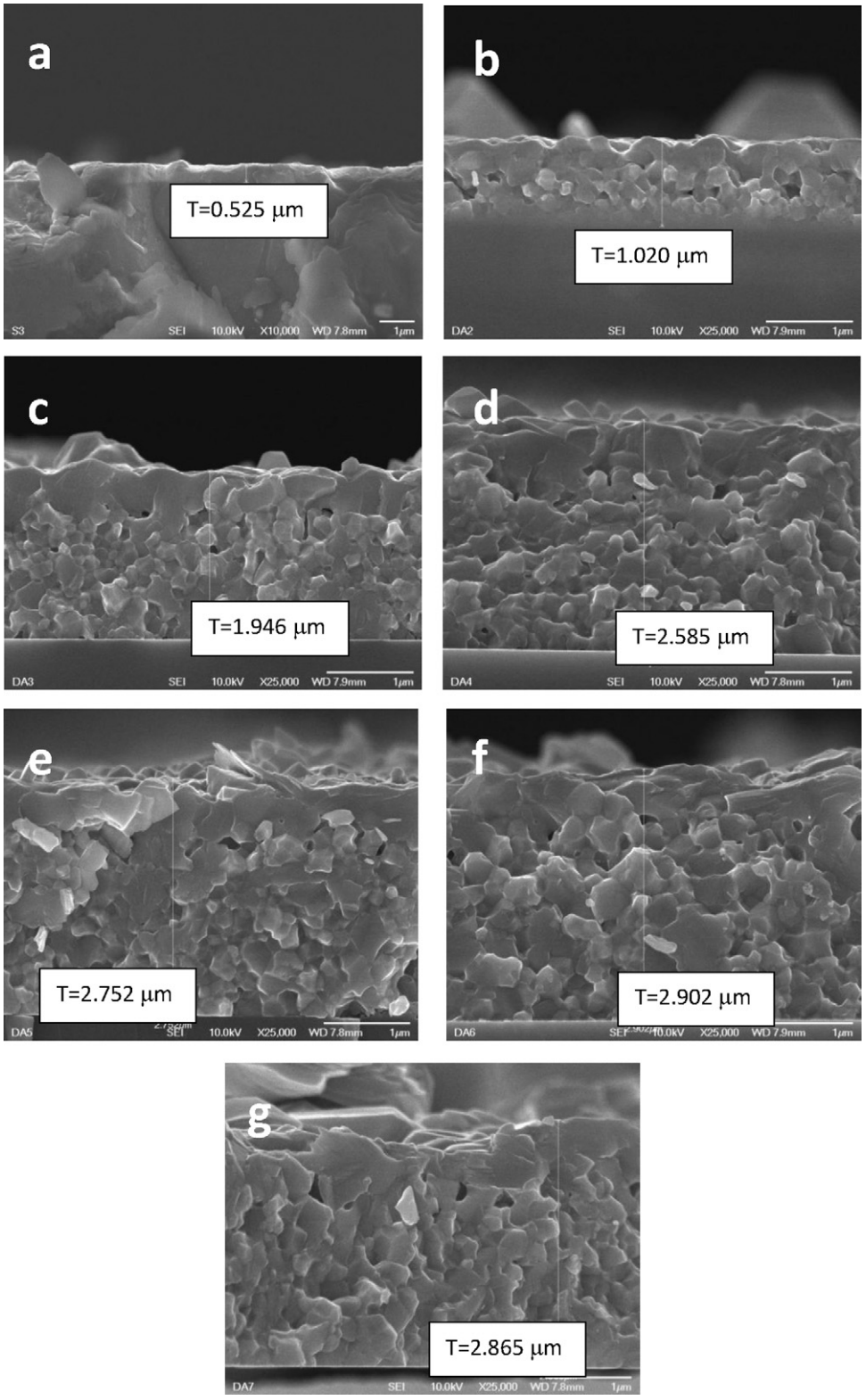

Fig. 4. Cross-sectional FE-SEM images of annealed CZTS thin films for various deposition times: (a) 5 min, (b) 10 min (c) 15 min, (d) 20 min, (e) 25 min, (f) 30 min and (g) 45 min.

and θ is Bragg's angle. Fig. 2 shows that the average crystallite size increases (15–31 nm) with increase in the deposition time up to 30 min and thereafter it decreases due to degradation of film.

The preferential crystallite orientation is obtained from different TCs $(h\,k\,l)$ defined by the well-known relation [25],

$$\mathrm{TC}(h\,k\,l) = \frac{I(h\,k\,l)/I_0(h\,k\,l)}{(1/N)\sum_N (I(h\,k\,l)/I_0(h\,k\,l))}$$

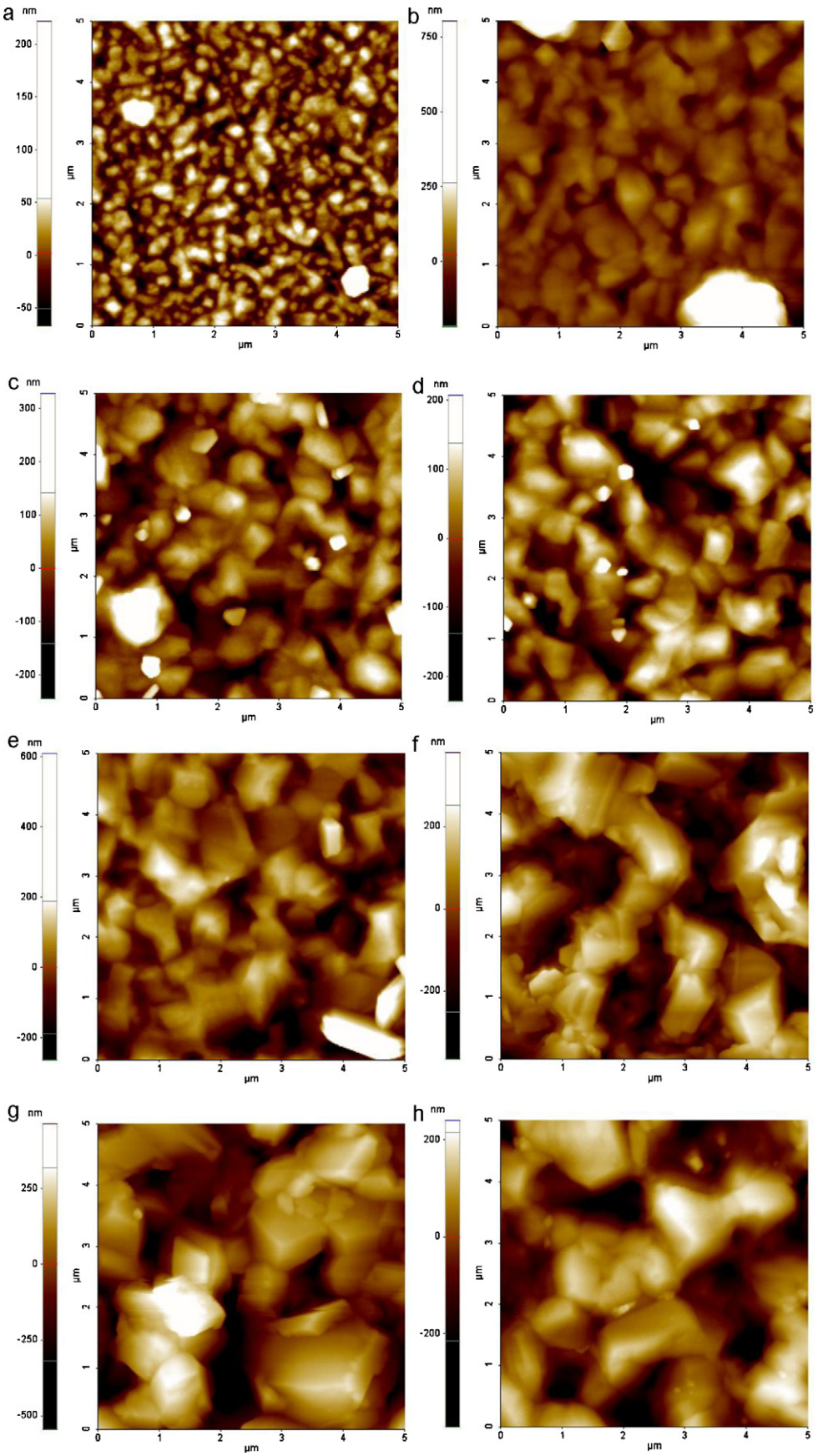

Fig. 5. AFM images of annealed CZTS thin films for various deposition times: (a) 5 min, (b) 10 min (c) 15 min, (d) 20 min, (e) 25 min, (f) 30 min, (g) 45 min and (h) 60 min.

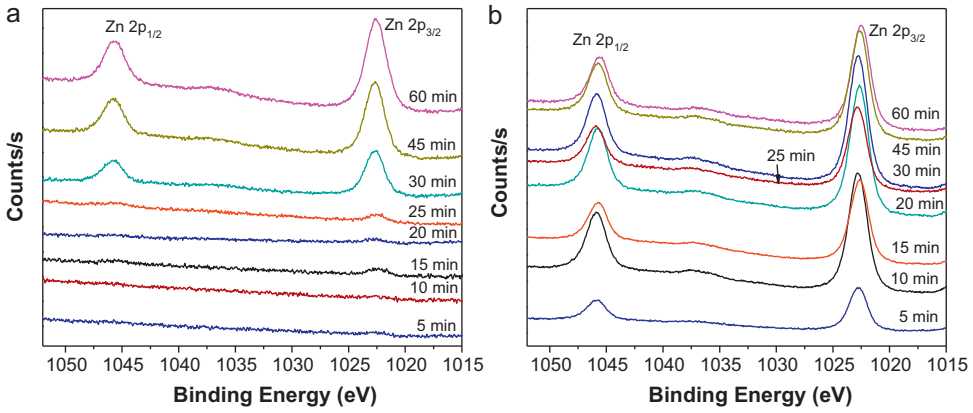

Fig. 6. The Zn 2p core level spectra of (a) as deposited (b) annealed CZTS thin films synthesized at various deposition times.

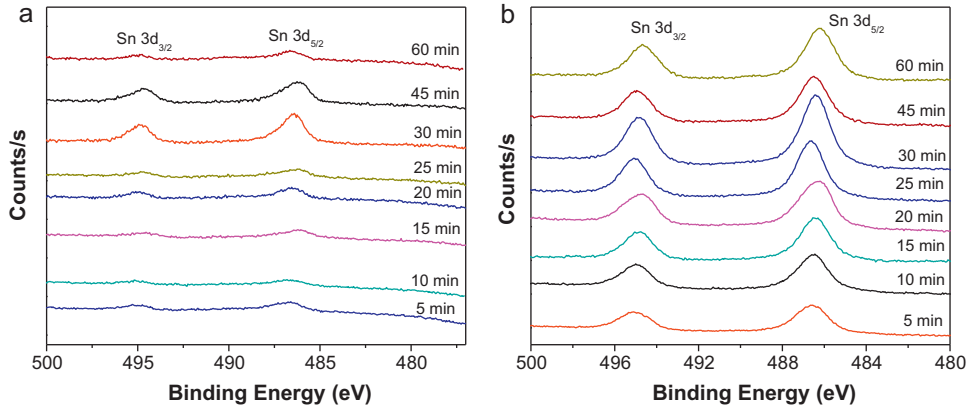

Fig. 7. The Sn 3d core level spectra of (a) as deposited (b) annealed CZTS thin films synthesized at various deposition times.

where TC is the texture coefficients of the (hkl) plane, I is the measured intensity, I_0 is the ASTM standard intensity and N is the reflection number. The TC along (1 1 2) orientation is larger than (3 1 2) and (2 2 0) orientations (Fig. 2). As the deposition time increases the TCs of all the planes upto 30 min increases while it decreases for higher deposition times. The observed changes in TC values can be attributed to the increase in extent of preferred orientation associated with the increased number of grains along (1 1 2) direction. The minimum interfacial energy may be the cause for the coalescence of grains as well as the rotation of preferred growth and can be ascribed to the observed variation of TC values.

3.1. Morphological analysis

Fig. 3(a–h) shows FE-SEM images of annealed CZTS thin films for various deposition times. It is observed that, due to recrystallization with annealing, resultant grain size is increased, compared to as-deposited film. However, severe porous feature including many voids are not observed in films. Deposited films are smooth, uniform, homogeneous and densely packed. Fig. 4(a–g) shows the cross-sectional FE-SEM images of the annealed CZTS thin films. The thickness of film is found to vary between 0.525 and 2.902 μm which indicates that deposition time is a vital parameter to increase the thickness indirectly to increase the efficiency. Thus

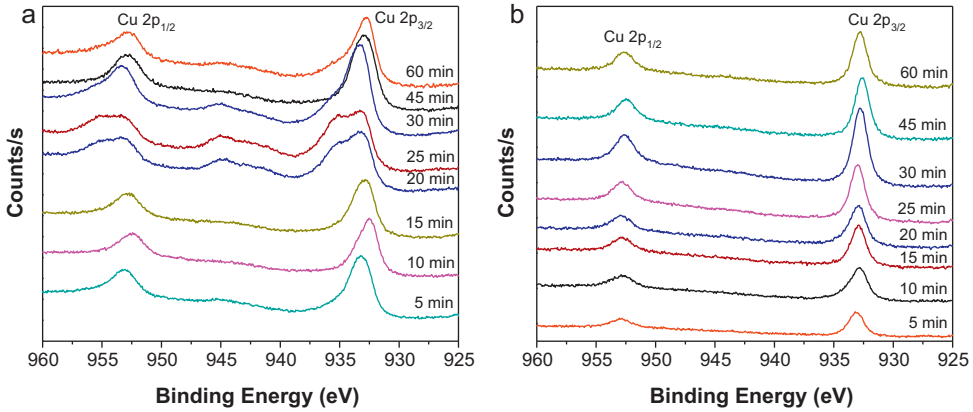

Fig. 8. The Cu 2p core level spectra of (a) as deposited (b) annealed CZTS thin films synthesized at various deposition times.

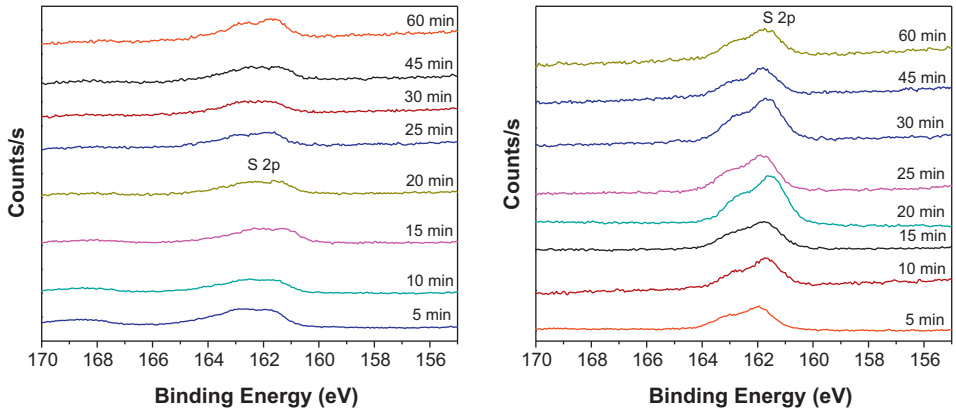

Fig. 9. The S 2p core level spectra of (a) as deposited (b) annealed CZTS thin films synthesized at various deposition times.

increase in appropriate deposition time is very desirable for high throughput production of CZTS based thin film solar cell. Fig. 5(a–h) shows 2D atomic force microscopy (AFM) images of annealed CZTS thin films. The roughness of the film increases up to 30 min and then decreases for higher deposition time (from 2 to 8 nm). The porosity (number of voids) of film decreases with deposition time. An improvement in crystallinity of the films with increase in film thickness is due to the ability of adatoms to move towards stable sites in the lattice, thereby favoring grain growth with preferred orientation. The film becomes more compact and devoid of pores when deposition time is increased to 30 min. This nature of the thicker films is attributed to tensile stress or strain generated in the film [26]. The foregoing discussion suggests that the variation of deposition time is the effective parameter to control the structure of CZTS thin films. Although the variation of this parameter is directly related with film thickness which is a material property, it is not straightforward to ascribe the change in structural properties to thickness for the following reasons. The present situation patent that the higher deposition time originates the change in phase of the material, which probably indicates that the acquired more thermal energy helps to diffuse the adatoms over the substrate surface and occupy a proper lattice position. It is established that the variation in deposition time affects the surface morphology of the films.

3.2. X-ray photoelectron spectroscopy

Fig. 6(a and b) shows the XPS core level spectra of Zn for as-deposited and annealed CZTS thin films. The spectra show well-resolved doublet of the Zn $2p_{3/2}$ and $2p_{1/2}$ components corresponding to 1022 and 1046 eV, for the deposited thin films. The binding energy of Zn $2p_{3/2}$ is attributed to the Zn^{2+} bonding state, which agrees well with the previous report [27]. Due to annealing of the films the core level intensity of Zn states increases. Fig. 7(a and b) shows the narrow scan XPS spectra of Sn $3d_{5/2}$ and Sn $3d_{3/2}$ of as-deposited and annealed CZTS thin films. The binding energies of $3d_{5/2}$ and $3d_{3/2}$ correspond to ~486 and 495 eV for as-deposited and annealed films respectively. The Sn 3d region consists of a single doublet at 495 eV for Sn $3d_{3/2}$ and 487 eV for Sn $3d_{5/2}$ due to so-called "final-state" effects. These binding energies are in good agreement with the reported values for Sn [28]. The binding energy of ~933and 953 eV can be ascribed to the Cu $2p_{3/2}$ and Cu $2p_{1/2}$ core levels as shown in Fig. 8(a and b). Broadening of the Cu $2p_{3/2}$ and Cu $2p_{1/2}$ has been observed after annealing in the $N_2 + H_2S$ atmosphere. The observed chemical shift is about ~20 eV, it slightly varies with deposition time and after annealing. Fig. 9(a and b) shows the doublet of the S present in the CZTS thin films. The binding energy around ~162 and 163 eV originated from the $2p_{3/2}$ and $2p_{1/2}$ electrons of S atoms. There is slight broadening in the S core levels due to annealing process.

3.3. Optical properties

Fig. 10 shows the variation $(\alpha h\nu)^2$ as a function of photon energy $(h\nu)$ for CZTS thin films deposited at typical deposition time 30 min for as deposited and annealed CZTS thin films. The energy dependent absorption coefficient can be expressed by the relation for the allowed direct transition as [29],

$$\alpha h\nu = A(h\nu - E_g)^{1/2}$$

where A is a constant, h is the Plank constant and E_g refers to the direct band gap. Based on the allowed direct inter band transition, the band gap is determined to be 1.67 and 1.54 eV by extrapolating the linear $(\alpha h\nu)^2$ vs. $h\nu$ plots to $(\alpha h\nu)^2 = 0$ for as-deposited and annealed films respectively. This is in agreement with band gaps reported for CZTS films [30]. This value is quite close to the theoretical optimal band gap value for a single-junction solar cell, and indicates that the CZTS film grown by PLD can be used as an absorber layer.

3.4. Device properties

Fig. 11(a) shows the J–V characteristics of the typical annealed CZTS-based solar cells deposited at 30 min. This annealed CZTS thin

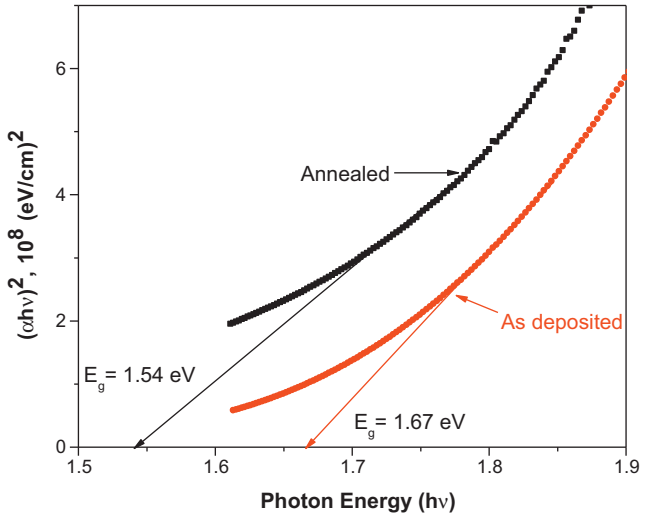

Fig. 10. Plot of $(\alpha h\nu)^2$ vs. $h\nu$ for as-deposited and annealed CZTS thin films for typical 30 min deposition time.

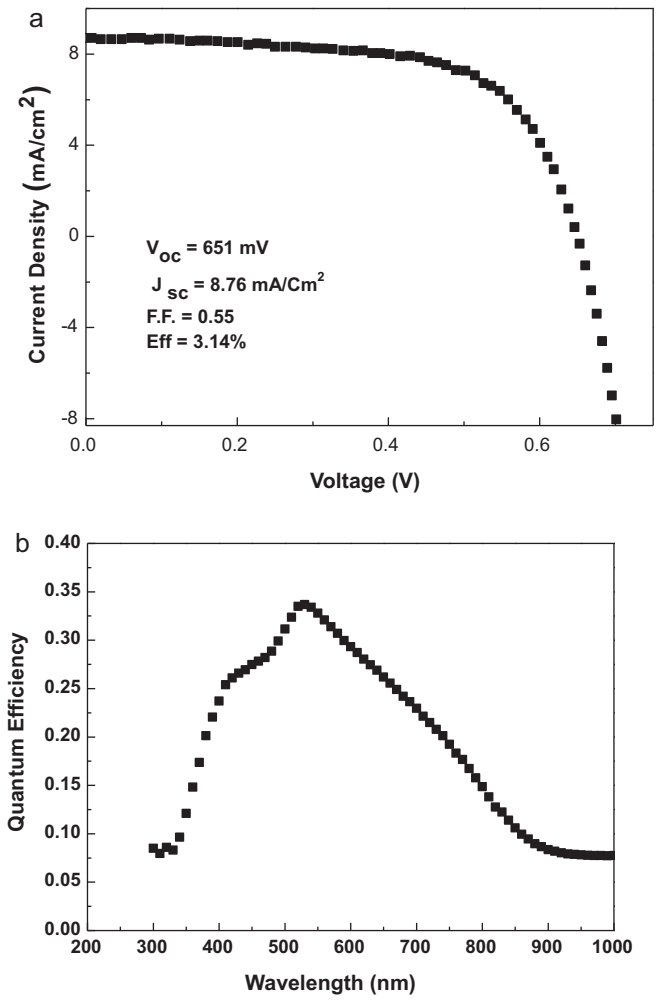

Fig. 11. (a) Photovoltaic output characteristic of solar cell formed with typical annealed CZTS (30 min deposition time) and chemical bath deposited CdS thin films (b) quantum efficiency w. r. t. wavelength for CZTS thin film deposited at 30 min deposition time.

film when used as an absorber layer in the solar cell configuration exhibits an open-circuit voltage (V_{oc}) of 651 mV, a short-circuit current (I_{sc}) of 8.76 mA/cm^2, a fill factor of 0.55, and a conversion efficiency of 3.14%. The enhanced efficiency of the solar cell is comparable to reported value [16,31]. The quantum efficiency 0.34% [Fig. 11(b)] shows peak at ~530 nm and then decreases monotonously with increase in the wavelength. The decrease in quantum efficiency at shorter wavelength side ($\lambda < 530$ nm) might be due to recombination of minority charge carriers at surface states. The spectrum shows the good configuration just like a trapezoid.

4. Conclusions

The effect of deposition time and annealing on to the physicochemical properties of nearly stoichiometric CZTS thin films grown by PLD has been investigated. Crystallinity of the film enhances with deposition time. Optical studies indicate that the CZTS film can be applied as an absorber layer for thin film solar cells. The conversion efficiency of 3.14% has been observed for glass/Mo/CZTS/CdS/ZnO:Al/Al thin film based solar cell.

Acknowledgments

A.V. Moholkar is grateful to the Department of Science and Technology (DST), New Delhi for awarding the BOYSCAST Fellowship (File No.SR/BY/P-02/2008) and University Grants Commission, New Delhi, India for the financial assistance through the minor research Project No F-47-707/2008. This work was supported by the National Research Foundation of Korea (NRF) grant funded by the Korea government (MEST) (K2080200147310B120004510).

References

[1] K. Ito, T. Nakazawa, Jpn. J. Appl. Phys. 27 (1988) 2094.
[2] Th.M. Friedlmeier, N. Wieser, Th. Walter, H. Dittrich, H.W. Schock, Proceedings of 14th European PVSEC and Exhibition, P4B, 1997, p. 10.
[3] R. Nitsche, D.F. Sargent, P. Wild, J. Cryst. Growth 1 (1967) 52.
[4] T. Tanaka, A. Yoshida, D. Saiki, K. Saito, Q. Guo, M. Nishio, T. Yamaguchi, Thin Solid Films 518 (2010) S29.
[5] C.P. Chan, H. Lam, C. Surya, Solar Energy Mater. Solar Cells 94 (2010) 207.
[6] X. Zhang, X. shi, w. Ye, C. Ma, C. Wang, Appl. Phys. A 94 (2009) 381.
[7] H. Yoo, J. Kim, Thin Solid Films 518 (2010) 6567.
[8] T. Tanaka, T. Nagatomo, D. Kawasaki, M. Nishio, Q. Guo, A. Wakahara, A. Yoshida, H. Ogawa, J. Phys. Chem. Solids 66 (2005) 1978.
[9] J.S. Seol, S.Y. Lee, J.C. Lee, H.D. Nam, K.H. Kim, Solar Energy Mater. Solar Cells 75 (2003) 155.
[10] K. Oishi, G. Saito, K. Ebina, M. Nagahashi, K. Jimbo, W.S. Maw, H. Katagiri, M. Yamazaki, H. Araki, A. Takeuchi, Thin Solid Films 517 (2008) 1449.
[11] A.V. Moholkar, S.S. Shinde, A.R. Babar, K.U. Sim, Y.B. Kwon, K.Y. Rajpure, P.S.Patil, C.H. Bhosale, J.H. Kim, Solar Energy, In Press, (2011).
[12] K. Moriya, K. Tanaka, H. Uchiki, Jpn. J. Appl. Phys. 47 (2008) 602.
[13] S.M. Pawar, A.V. Moholkar, I.K. Kim, S.W. Shin, J.H. Moon, J.I. Rhee, J.H. Kim, Curr. Appl. Phys. 10 (2010) 565.
[14] H. Katagiri, K. Saitoh, T. Washio, H. Shinohara, T. Kurumadani, S. Miyajima, Solar Energy Mater. Solar Cells 65 (2001) 141.
[15] Y.B. Kishore Kumar, G. Suresh Babu, P. Uday Bhaskar, V. Sundara Raja, Solar Energy Mater. Solar Cells 93 (2009) 1230.
[16] K. Tanaka, M. Oonuki, N. Moritake, H. Uchiki, Solar Energy Mater. Solar Cells 93 (2009) 583.
[17] B. Kramer (Ed.), Adv. Solid State Phys. 43 (2003) 505.
[18] D.B. Chrisey, G.K. Hubler (Eds.), Pulsed Laser Deposition of Thin Films, John Wiley and Sons, New York, 1994.
[19] C. Belouet, Appl. Surf. Sci. 96 (1996) 630.
[20] K.D. Develos, M. Kusunoki, M. Mukaida, S. Ohshima, Physica C 320 (1999) 21.
[21] R. Aguiar, V. Trtik, F. Sfinchez, C. Ferrater, M. Varela, Thin Solid Films 304 (1997) 225.
[22] J.W. Moon, N. Wakiya, K. Fujito, N. Iimori, T. Kiguchi, T. Yoshika, J. Tanaka, K. Shinozaki, Mater. Sci. Eng. B 148 (2008) 22.
[23] K.U. Sim, S.W. Shin, A.V. Moholkar, J.H. Yun, J.H. Moon, J.H. Kim, Curr. Appl. Phys. 10 (2010) S463.
[24] Q. Guo, H.W. Hillhouse, R. Agrawal, J. Am. Chem. Soc. 131 (2009) 11672.
[25] A.R. Babar, P.R. Deshamukh, R.J. Deokate, D. Haranath, C.H. Bhosale, K.Y. Rajpure, J. Phys. D: Appl. Phys. 41 (2008) 135404.
[26] S.S. Shinde, P.S. Shinde, C.H. Bhosale, K.Y. Rajpure, J. Phys. D: Appl. Phys. 41 (2008) 105109.
[27] S.S. Shinde, P.S. Shinde, V.G. Sathe, S.R. Barman, C.H. Bhosale, K.Y. Rajpure, J. Mol. Struct. 984 (2010) 186.
[28] A.R. Babar, S.S. Shinde, A.V. Moholkar, K.Y. Rajpure, J. Alloys Compd. 505 (2010) 743.
[29] J. Tauc, F. Abeles (Eds.), Optical Properties of Solids, North Holand, Amsterdam, 1970.
[30] J.J. Scragg, P.J. Dale, L.M. Peter, Thin Solid Films 517 (2009) 2481.
[31] H. Araki, A. Mikaduki, Y. Kubo, T. Sato, K. Jimbo, W.S. Maw, H. Katagiri, M. Yamazaki, K. Oishi, A. Takeuchi, Thin Solid Films 517 (2008) 1457.